Chin. Geogra. Sci. 2023 Vol. 33 No. 1 pp. 131−143
https://doi.org/10.1007/s11769-022-1324-y

Springer Science Press
www.springerlink.com/content/1002-0063

Surface Regional Heat (Cool) Island Effect and Its Diurnal Differences in Arid and Semiarid Resource-based Urban Agglomerations

CHEN Yan, XIE Miaomiao, CHEN Bin, WANG Huihui, TENG Yali

(*School of Land Science and Technology*, *China University of Geosciences*, *Beijing* 100083, *China*)

Abstract: With the rapid development of urban agglomerations in northwest arid and semiarid regions of China, the scope of the urban heat island (UHI) effect has gradually expanded and gradually connected, and has formed a regional heat island (RHI) with a larger range of impact to the regional environment. However, there are few studies on the heat island effect of urban agglomerations in arid and semiarid regions, so this paper selects the urban agglomeration of Hohhot, Baotou and Ordos (HBO) of Inner Mongolia, China as the study area. Based on the 8-day composite Moderate-resolution Imaging Spectroradiometer (MODIS) surface temperature data (156 scenes in all) and land use maps for 2005, 2010, and 2015, we analyze the spatiotemporal distributions of regional heat (cool) islands (RH(C)I) and the responses of surface temperatures to land-use changes in the diurnal and interannual surface cities. The results showed that: 1) from 2005 to 2015, urban areas showed the cold island effect during the day, with the area of the cold island showing a shrinking feature; at night, they showed the heat island effect, with the area of the heat island showing a first decrease and then an increase. 2) From 2005 to 2015, the land development (unutilized land to building land) brings the greatest temperature increase (ΔT = 1.36°C) during the day, while the greatest temperature change at night corresponds to the conversion of cultivated land to building land (ΔT = 0.78°C) exhibited the largest changes at night. From 2010 to 2015, the land development (grassland to building land) bring the greatest temperature increase (ΔT = 0.85°C) during the day, while the great temperature change at night corresponds to the conversion of water areas to building land (ΔT = 1.38°C) exhibited the largest changes at night. Exploring the spatial and temporal evolution of surface urban heat (cool) islands in urban agglomerations in arid and semiarid regions will help to understand the urbanization characteristics of urban agglomerations and provide a reference for the formulation of policies for the coordinated and healthy development of the region and co-governance of regional environmental problems.

Keywords: regional heat (cool) island (RH(C)I); urban agglomeration; arid and semiarid areas; land-use change; land surface temperature (LST)

Citation: CHEN Yan, XIE Miaomiao, CHEN Bin, WANG Huihui, TENG Yali, 2023. Surface Regional Heat (Cool) Island Effect and Its Diurnal Differences in Arid and Semiarid Resource-based Urban Agglomerations. *Chinese Geographical Science*, 33(1): 131−143. https://doi.org/10.1007/s11769-022-1324-y

1 Introduction

Due to rapid economic development, the scales of urban areas continue to expand globally (UN-Habitat, 2016). Urbanization has caused many rural people to gather in cities, so this has led to a surge in demand for construction land and a dramatic change in the land cover structure (Seto et al., 2012). By 2030, more than half of the world's new urban areas will be located in Asia and by 2050, the total urban population will account for 68% of the total population, with the majority living in Asia and Africa (United Nations, 2018). Changes in ground cover, urban structures and building surface materials cause changes in the balance of radiant energy at

Received date: 2021-11-30; accepted date: 2022-04-01
Corresponding author: XIE Miaomiao. E-mail: xmiaomiao@gmail.com

the surface and result in higher urban surface temperatures (Oleson et al., 2015; Sun et al., 2019; Yu et al., 2019a). The resulting urban heat island effect (UHI) is detrimental to air quality, health of residents, and energy consumption (Debbage and Shepherd, 2015; Fu and Weng, 2016; Peng et al., 2016), which is a challenge for sustainable development in developing countries.

Since UHIs were proposed, scholars have analyzed and researched the formation mechanisms, characteristics of the evolution patterns, driving factors, and mitigation methods of individual UHIs (Stewart, 2011; Akbari and Kolokotsa, 2016), and numerous research results have made great contributions to mitigating UHIs in individual cities. However, with the accelerated urbanization process, the city scales have been expanding. Large-scale urban agglomerations form among cities with close geographic locations and economic relationships, and they have become a development trend (Gao et al., 2019; Yuan et al., 2019; Li et al., 2020; Wang et al., 2020b). Compared with individual cities, the conflict between urbanization development and ecological environment is more intense in urban agglomerations, which makes urban agglomerations gradually become a concentrated region of ecological and environmental problems (Fang et al., 2016). Under the development of urban agglomerations, urban-rural boundaries are gradually weakening and then dramatically change the thermal environment in continuous areas (Du et al., 2016; Zhou et al., 2016; Yu et al., 2019b). The development of urban agglomerations has caused the urban heat island problem to no longer be limited to individual cities, and this problem has gradually expanded to the regional level, with urban heat islands between cities gradually connecting to form regional heat islands (RHI) with a larger impact to the environment (Gao et al., 2019; Yuan et al., 2019; Liao et al., 2021; Wang et al., 2020a). In recent years, China has vigorously promoted the development of urban agglomerations to drive regional economic growth, and among them, several urban agglomerations are distributed in the arid and semiarid regions of northwest China. The fragile ecological environment in arid and semiarid regions is more vulnerable to the urbanization process, which hinders the healthy development of urban agglomerations in arid and semiarid regions (Song et al., 2020). Therefore, it is necessary to study the RHI of urban agglomerations in arid and semiarid regions to understand its distribution characteristics and evolution patterns.

The study of RHI in urban agglomerations mostly focuses on the morphological changes and influencing factors of heat islands, and the study areas are mostly located in the eastern coastal region of China, such as the Yangtze River Delta urban agglomeration and the Pearl River Delta urban agglomeration. For example, Ge et al. (2010) analyzed the RHI distribution characteristics of the Yangtze River Delta urban agglomeration through GIS geostatistical methods, and pointed out that the heat island distribution of major cities showed a 'Z' pattern, with the strongest heat island in summer, followed by spring, and weak or no heat island in most areas in autumn and winter. Wu et al. (2021) analyzed the effects of socioeconomic, urban agglomeration and physical indicators on RHI in the Pearl River Delta urban agglomeration and found that physical factors are the determinants of regional heat islands during daytime, while socioeconomic factors are the determinants of regional heat islands at night. There are still few studies on RHI in urban agglomerations and almost no studies on RHI in urban agglomerations in arid and semiarid regions. Most of the UHI studies based on arid and semiarid regions are at the individual city scale, and investigate the diurnal (Jahangir et al., 2019; LemoineRodrguez et al., 2022) and seasonal (Haashemi et al., 2016; Quintanatalvac et al., 2021) UHI variation patterns and has explored the effects of land surface temperature (LST) estimation methods (Majumder et al., 2021), land use cover (Haashemi et al., 2016), and others on UHIs. The UHIs in arid and semiarid regions have some differences from other regions, such as exhibiting a typical urban cool island during the day, i.e., the urban core appears cooler when compared to suburban and rural areas (Lazzarini et al., 2013; Rasul et al., 2017; Mohammad et al., 2019; Wu et al., 2019), which can be attributed to the evaporative cooling caused by urban vegetation and soil moisture (Peng et al., 2012; Lazzarini et al., 2013). In contrast, at night, the urban core exhibits an urban heat island due to the heat release from roads as well as buildings due to the albedo, evapotranspiration and refractive index, which results in higher LSTs than in the suburbs (Taha, 1997; Bonafoni et al., 2017; Luintel et al., 2019). There are few studies in the existing literature that focus on UHIs in arid and semiarid regions (Yun et al., 2020), even if they also suffer from negat-

ive effects (Quintanatalvac et al., 2021). The heat island effect of urban agglomerations in arid and semiarid regions has received less attention, but the healthy development of urban agglomerations is extremely important for the regional economy. Therefore, it is necessary to explore the characteristics of RHI in urban agglomerations in arid and semiarid regions from a regional perspective, so as to provide a reference basis for urban planning at the regional level.

The urban agglomeration of Hohhot, Baotou and Ordos (HBO) of Inner Mongolia, China is an emerging urban agglomeration, as a regional urban agglomeration in the central and western region of the 'Two Horizontal and Three Vertical' strategic planning pattern of China's main functional area, it is an important growth pole for the coordinated development of the central and western region, and has an important role in the development of the regional economy. HBO urban agglomeration plays an important role in the development of regional economy. The study of the RHI of the HBO urban agglomeration is important for the future development planning of the urban agglomerations in arid and semiarid regions. In this paper, the HBO urban agglomeration is selected as the study area. By using data from the years 2000, 2010 and 2015, a total of 156 scenes of the MOD11A2 surface temperature data and land use and cover data were used. The effects of interannual diurnal regional heat island intensities and land-use changes on the surface temperature changes in the HBO urban agglomeration were analyzed. This research aimed to obtain: 1) the distribution differences and regularities of day and night surface regional heat (cool) islands in arid and semiarid urban agglomerations. 2) the impacts of land-use changes on surface temperatures. It provides a reference for the ecological environmental protection of the HBO urban agglomeration, optimizes the layout of towns and promotes the construction of a regional ecological civilization to promote the harmonious and healthy development of the region.

2 Materials and Methods

2.1 Study area

The HBO urban agglomeration includes Hohhot, Baotou and Ordos of Inner Mongolia in China (Fig. 1). The geographical location lies between 37°35′N–42°40′N and 106°42′E–112°10′E, with a total area of 131 600 km^2, which accounts for 11.4% of the land area of the entire Inner Mongolia Autonomous Region. Hohhot City is located on the Tumochuan Plain in central Inner Mongolia and borders the Yellow River and Daqing Mountain to the north; Baotou City is located at the southern end of the Mongolian Plateau and is bordered by the Tumochuan Plain and Hetao Plain to the east and west,

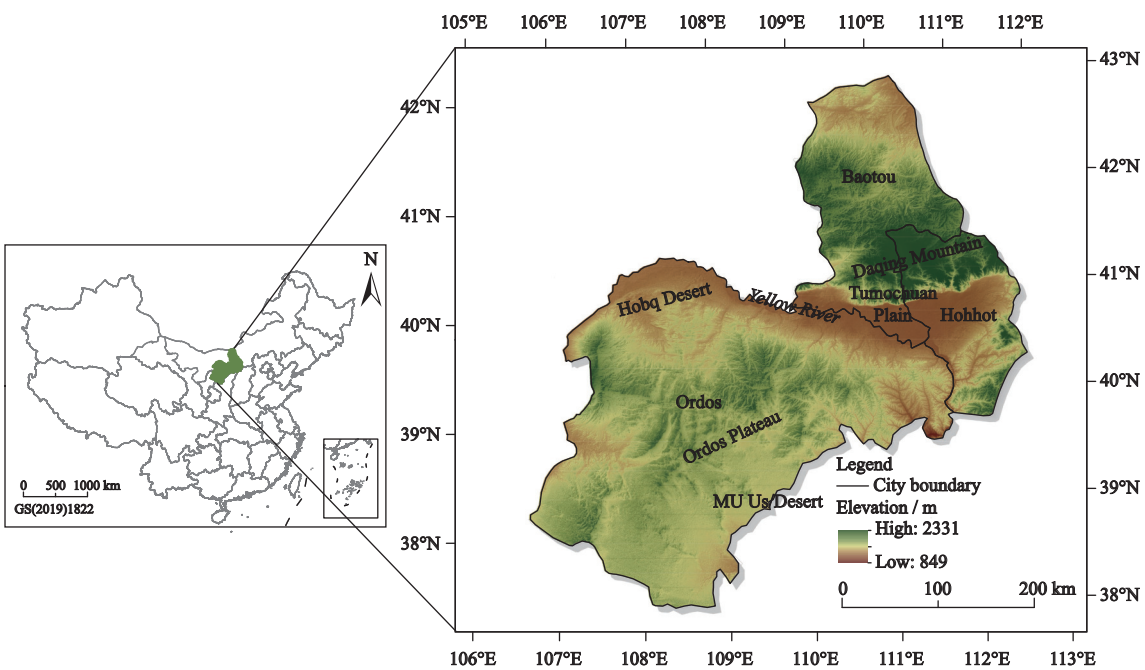

Fig. 1 Location of the HBO (Hohhot, Baotou and Ordos) urban agglomeration in China

respectively, and is bordered by the Yellow River to the south; Ordos City is located in the hinterland of the Ordos Plateau. The study area consists of an arid and semiarid regions with a semiarid continental monsoon steppe climate. In spring, it is relatively dry and windy, with drastic changes between cold and warm temperatures; summer is hot with little precipitation; in autumn, the temperatures drop rapidly, and the area is prone to frost; in winter, it is cold, which persists for a long time.

The HBO urban agglomeration belongs to the experimental area for the sustainable development of the national resource-based urban area, national energy and mineral resource enrichment area and economic development core area of Inner Mongolia. In 2015, the permanent residential population of the three cities was 7.934 million, which accounted for 31.6% of the permanent population of the Inner Mongolia Autonomous Region. Moreover, the GDP was 1103.858 billion yuan (RMB), which accounted for 53.69% of the total for the Inner Mongolia Autonomous Region (Inner Mongolia Autonomous Region Statistics Bureau, 2016).

2.2 Data and methods

2.2.1 Data sources and processing

(1) Moderate-resolution Imaging Spectroradiometer (MODIS) data. This study uses the MOD11A2 dataset, an 8-day composite land surface temperature (LST) products that is available on National Aeronautics and Space Administration's official website (https://lpdaac.usgs.gov/) to extract the surface temperatures and then analyzes the day-night changes in the RHI in the urban agglomeration. The dataset is generated by the MODIS/Terra space instrument and has significant advantages over other datasets and is widely used in regional- and global-scale UHI studies (Yao et al., 2017). MOD11A2 is a level 3 product with a resolution of 1 km. Based on the 1B data, it corrects the edge distortions in the images, so image corrections can be omitted during preprocessing. This dataset can provide surface temperature data during the daytime (10:30 a.m.) and nighttime (10:30 p.m.), which are in the process of surface temperature increase and decrease respectively (Qiao and Tian et al., 2015), and can satisfy the requirements for studying interannual RHIs. The period of 2000–2015 is the stage of rapid urbanization process of HBO urban agglomeration (Zhuang et al., 2019), and numerous studies have shown that there is a strong link between urbanization process and heat islands (Yuan et al., 2019; Yu et al., 2019b; Liao et al., 2021), so the period of 2000–2015 is more suitable for this paper to study the generation of regional heat island due to urbanization. However, due to the large range of missing values in the year 2000, using data from that year may have an impact on the results. Therefore, based on the research content, this study selects the MOD11A2 data (46 images per year) from 2005, 2010 and 2015, calculates the day and night annual averages in ArcGIS, and then calculates the Regional Heat Island Intensity (RHII).

(2) Land use cover data. This dataset is provided by the Data Center for Resources and Environmental Sciences, Chinese Academy of Sciences (RESDC) (http://www.resdc.cn). We chose the land use cover data of 2005, 2010 and 2015 with a resolution of 1 km. There are 25 land-use types in this dataset, which were reclassified into six types for the convenience of research, namely, cultivated land, forestland, grassland, water area, building land and unutilized land. We use the reclassified data to create a land use transfer matrix. After that, the land use cover data and LST data can be spatially linked. The statistics of the LSTs and their changes in each class were used in Excel and were used to analyze the impact of land use transfers on the LSTs.

(3) Digital Elevation Model (DEM) data. This elevation dataset area provided by the Data Center for RESDC (http://www.resdc.cn). Elevation data can help to extract plain areas and reduce the calculation errors that are caused by large terrain differences.

(4) Night light data. This study uses the 2013 DMSP/OLS night light dataset to help extract the areas that are less affected by human activities to obtain the final rural background. These data were obtained from the National Environmental Information Data Center of the National Aeronautics and Space Administration (http://ngdc.noaa.gov/eog/dmsp).

2.2.2 Regional Heat Island Intensity (RHII) calculation

In ArcGIS, the eight-day composite MOD11A2 data from 2005, 2010 and 2015 were calculated by using the raster calculator to determine the average values that are used to obtain the day and night interannual average LST data. The DEM elevation data, land use cover data and night light data were used to extract the rural background area, the RHII of the study area was obtained by using the regional heat island intensity calculation for-

mula (Yu et al., 2019b). However, the cold island range is not defined in the class classification, so combined with the results of RHII calculation, the RHII of HBO urban agglomeration is divided into five levels, and the range levels for the RHIIs for each level were as follows: Strong Cool Island, < –1°C; Weak Cool Island, –1–0°C; No Heat Island, 0–2°C; Weak Heat Island, 2–3°C; and Strong Heat Island, > 3°C. The formula is as follows (Eq. (1)):

$$RHII_i = T_i - \frac{1}{n}\sum_{1}^{n} T_{\text{crop}} \quad (1)$$

In this formula, $RHII_i$ refers to the *RHII* of pixel *i* in the remote sensing image (°C), T_i is LST of pixel *i* (°C), and *n* is the number of selected rural background pixels. T_{crop} represents the rural background pixel LST (°C) that eliminates the influences of terrain, water bodies and human activities.

Rural background extraction refers to the method proposed by Liu et al. (2017), using data from 2015 to extract four indicators of plain area, cropland type, night light value and NDVI value for overlay, and the obtained rural background was used for RHII calculation in 2005, 2010, and 2015. However, the HBO urban agglomeration is located in a semiarid region with low vegetation cover, so three indicators other than the NDVI were selected as overlays to obtain the final rural background.

(1) Plain area extraction. Excessive terrain height differences will cause certain errors in heat island intensities. The DEM data are used to extract those areas with elevation differences of ≤ 50 m from the built-up area, which can eliminate the heat island intensity errors that are caused by terrain differences and make the results more accurate (Fig. 2a).

(2) Night light values. Human activity is an important influencing factor of the heat island effect, so this paper extracts those pixels with night light values ≤ 15 to eliminate areas with excessive human interference (Fig. 2b). The DMSP/OLS sensor functions at night and can detect low-intensity light that is emitted by city lights, even small-scale residential areas, and traffic flow, and can distinguish this light from the dark rural background. Therefore, night light images can be used as a representation of human activity and can be a good data source for research on human activity monitoring.

(3) Cultivated land type extraction. The study area is located in an arid and semiarid region, and most of the cultivated land is dry land. Therefore, this paper uses land use classification data and reclassifies the land types into building land, water area, cultivated land, grassland, forestland and unutilized land to extract the cultivated land for the final rural background extraction (Fig. 2c).

By using the above three indicators, we can determine rural background areas with research resolutions of 1 km (Fig. 2d).

2.2.3 Responses of surface temperature to land-use changes

Urbanization is the main cause of land-use type changes, among which the expansion of building land is one of the important features of urbanization. Analyzing the LST characteristics of the land use types and responses of the LSTs to the expansion of building land can help us to understand the relationship between the thermal environment and land-use changes during urbanization.

Therefore, in this study, the diurnal annual average

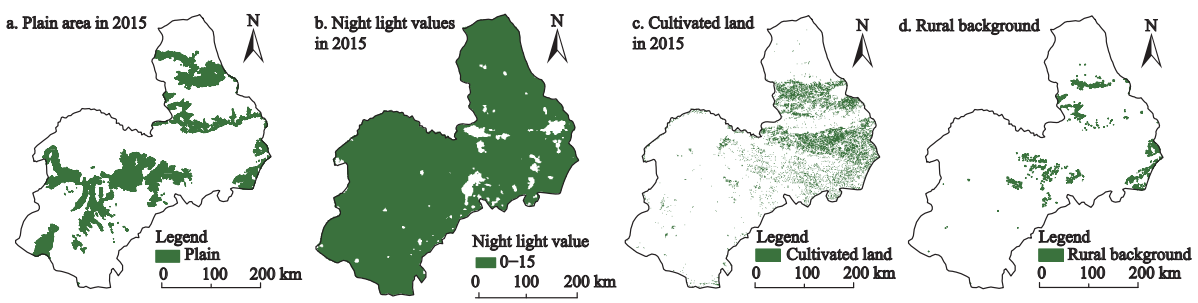

Fig. 2 (a) Plain area extraction with urban DEM differences ≤ 50 m; (b) area extraction with night light values ≤ 15; (c) cultivated land extraction based on land cover data; and (d) final rural background obtained by overlaying the first three images in HBO urban agglomeration of China

surface temperature data from 2005 to 2015 in the study area were overlaid with the land use classification data by using ArcGIS software. The statistics were generated in Excel to obtain the surface temperatures of each land-use type. Moreover, by using the land-use classification data from 2005 to 2015, land-use transfer matrices from 2005 to 2010 and from 2010 to 2015 were produced, and by overlaying the interannual surface temperature differences, the categories of land conversion to building land from 2005 to 2010 and from 2010 to 2015 (e.g., cultivated land to building land, forestland to building land, grassland to building land, water area to building land, building land to building land, and unutilized land to building land), the characteristics of the LST changes when different land-use types were converted to building land were analyzed. The land-use transformation matrix can reflect the dynamic process of inter-conversion between the area of each type at the beginning and at the end of a period of time in a region, and it has the generic form of (Eq. (2)):

$$S_{ij} = \begin{bmatrix} S_{11} & S_{12} & \cdots & S_{1n} \\ S_{21} & S_{22} & \cdots & S_{2n} \\ \cdots & \cdots & \cdots & \cdots \\ S_{1n} & S_{2n} & \cdots & S_{nn} \end{bmatrix} \quad (2)$$

where S_{ij} refers to area of land-use type i converted to land-use type j. n refers to the number of land-use types.

3 Results

3.1 Day and night regional heat (cool) island intensities

From the spatial distribution of Regional Heat (Cool) Island (RH(C)I) in Hohhot, Baotou and Ordos (HBO) urban agglomeration, during the daytime, cold islands are mainly distributed in the eastern, northern and central areas, and heat islands are mainly distributed in the desert areas in the west and southwest (Fig. 3). At night, cold islands are mainly distributed in the northern and central-western regions of the urban agglomeration, and heat islands are mainly distributed in the central, northwestern and southern regions (Fig. 4). The southern and northwestern parts of the urban agglomeration are distributed with the Mu Us Desert and Hobq Desert, which show heat island effect due to their own arid climate effects, with higher daytime and nighttime temperatures than the rural background temperature. The central and eastern parts of the urban agglomeration are densely distributed areas of building land (Fig. 5). The densely distributed areas of building land in the central of the urban agglomeration show Weak Cool Island and Strong Cool Island in general, and Weak Cool Island in the eastern; while the densely distributed areas of construction land in the central of the urban agglomeration show Weak Heat Island and Strong Heat Island at night, and Weak Heat Island effect in the eastern. Most of the densely building land areas are urban areas, which have relatively good greening facilities compared with rural areas. The high level of vegetation coverage can cool down the temperatures during the day and at night can also retain the heat released from building land. In contrast, there are more bare lands and low-coverage grasslands in the suburbs, and the overall vegetation coverage is low. These land types with low vegetation cover have the characteristics of rapid heating during the day and rapid cooling at night. As a result, the land surface temperature (LST) of the densely built land areas during the day are lower than those of the suburbs and exhibit a cold island effect, and the LSTs at night are higher than those of the suburbs and show a heat island effect. It is inferred from these observations that the land

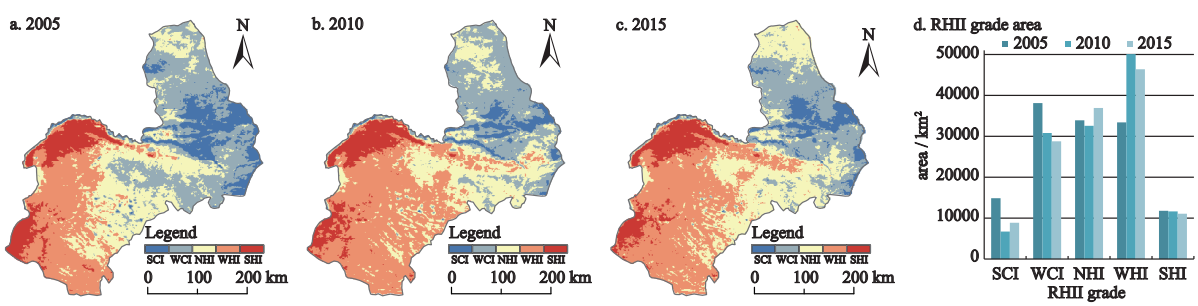

Fig. 3 Intensity distributions and areas of regional heat (cool) islands (RH(C)I) in the daytime from 2005–2015 in HBO urban agglomeration, China. SCI (Strong Cool Island); WCI (Weak Cool Island); NHI (No Heat Island); WHI (Weak Heat Island); SHI (Strong Heat Island); RHII (regional heat island intensity)

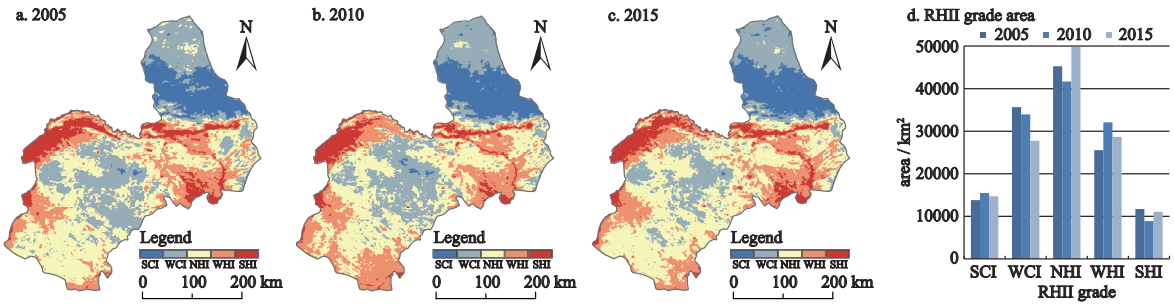

Fig. 4 Intensity distributions and areas of regional heat (cool) islands (RH(C)I) at night from 2005–2015 in HBO urban agglomeration, China. SCI (Strong Cool Island); WCI (Weak Cool Island); NHI (No Heat Island); WHI (Weak Heat Island); SHI (Strong Heat Island); RHII (regional heat island intensity)

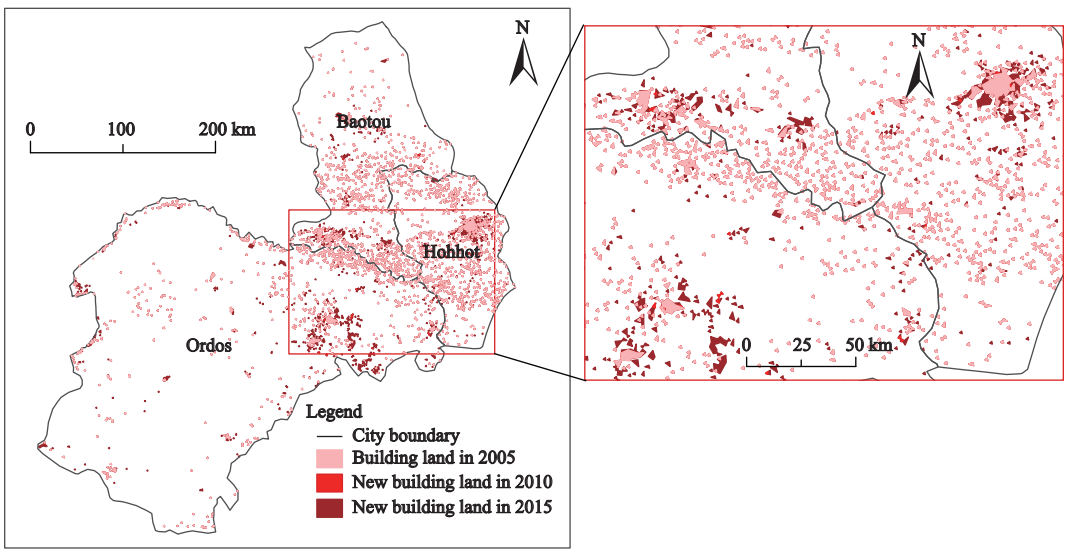

Fig. 5 Changes of building land from 2005–2015 in HBO urban agglomeration, China

use cover type is a significant factor that leads to cool islands during the day and heat islands at night. Additionally, we found that the distribution of building land to the north of Daqing Mountain also had a larger area but showed both strong and weak cool island effects during the day and night. Because the building land in the north is relatively scattered and the elevations are higher in the north, this area does not exhibit the heat island effect at a regional scale; the barrier of Daqing Mountain causes the building areas in the north and central parts of the study area to not be connected into one piece and thus produces differences.

From the area change of RH(C)I in HBO urban agglomeration (Fig. 3d, Fig. 4d). During the daytime from 2005 to 2015, the Strong Cool Island range of HBO urban agglomeration showed the characteristics of shrinkage before expansion, with the areas of 14 846.42, 6697.86 and 8874.43 km^2 in 2005, 2010 and 2015, respectively. Weak Cool Island range showed the characteristics of shrinkage year by year, with the areas of 38 112.75, 30 793.36 and 28 758.21 km^2 in above three years, respectively. The scope of No Heat Island showed a small shrinkage followed by a large expansion, with an area of 33 917.62, 32 5973.28 and 36 931.10 km^2 in each year, respectively. The scope of Weak Heat Island showed a large expansion followed by a small shrinkage, with an area of 33 395.77, 50 086.08, 46 393.44 km^2. Strong Heat Island range shows the characteristics of gradual and small shrinkage, with the areas of 11 770.07, 11 633.53, 11 066.54 km^2 in each year, respectively. During the night from 2005 to 2015, the urban agglomeration Strong Cool Island range was characterized by expansion followed by a small shrinkage, with the areas of 13 820.22 km^2, 15 473.43 km^2 and 14 741.91 km^2 in 2005, 2010 and 2015, respectively. Weak Cool Island range was characterized by gradual shrinkage, with the

areas of 35 666.94, 33 942.47 and 27 749.10 km^2 in each year, respectively. The No Heat Island range is characterized by a shrinkage followed by a large expansion, with the areas of 45 270.35, 41 666.65 and 49 787.49 km^2 in each year, respectively; the Weak Heat Island range is characterized by a large expansion followed by a small shrinkage, with the areas of 25 549.33, 32 077.31 and 28 672.58 km^2 in each year, respectively; the Strong Heat Island range is characterized by a shrinkage followed by an expansion, with the areas of 11 709.71, 8883.46 and 11 074.04 km^2 in each year, respectively.

In Fig. 3 and Fig. 4, we can see that the extent of the Weak Heat Island in the west and south during the daytime and the extent of the Strong Cool Island in the three urban junction areas in the central part change the most; the extent of the weak heat island in the south and the strong heat island in the central part change greatly at night. The diurnal regional heat island effect in the three urban junction areas in the central part of the urban agglomeration changed significantly from 2005 to 2015. At the same time, the central part is a densely distributed area for building land, and we reasonably speculate that the distribution and evolution characteristics of RH(C)I in the HBO urban agglomeration are more influenced by urbanization.

3.2 Response of surface temperature to land-use changes

3.2.1 Day and night surface temperatures of different land-use types

The LSTs of grassland and building land during the daytime from 2005 to 2015 decreased first and then increased (Fig. 6a), while the LSTs for the other land types gradually increased. Additionally, grassland had the highest LSTs, which were followed by unutilized land, while forestland had the lowest LSTs. In the nights from 2005 to 2015, the LSTs of each class exhibited year by year increases. The LSTs of building land were the highest, which were followed by water area and unutilized land; the LSTs of cultivated land were the lowest (Fig. 6b). It can also be seen from the chart that when compared with 2005 and 2010, the LSTs of each class were highest in 2015.

In general, unutilized land has high LSTs during both the day and night and belongs to high-temperature land; grassland is high-temperature land during the day and low-temperature land at night; building land and water areas are relatively low-temperature land during the day and night; the land types with low temperatures during the day and night are cultivated land and forestland.

3.2.2 Response of surface temperatures to construction land changes

It can be seen from Table 1 that, from 2005 to 2010, the most significant increases in LSTs (ΔT = 1.36°C) were observed during the daytime when unutilized land which is mainly marshland with the low LSTs was converted to building land. Additionally, the LSTs changes that were due to the conversion of cultivated land to building land exhibited decreases because the cultivated land around the cities is mainly fallow land. The surface vegetation cover of fallow land is very poor, so it has higher LSTs than building land. At night, the LSTs increased after the conversion of each land type to building land. The changes in LSTs that were due to the conversion of cultivated land to building land were the

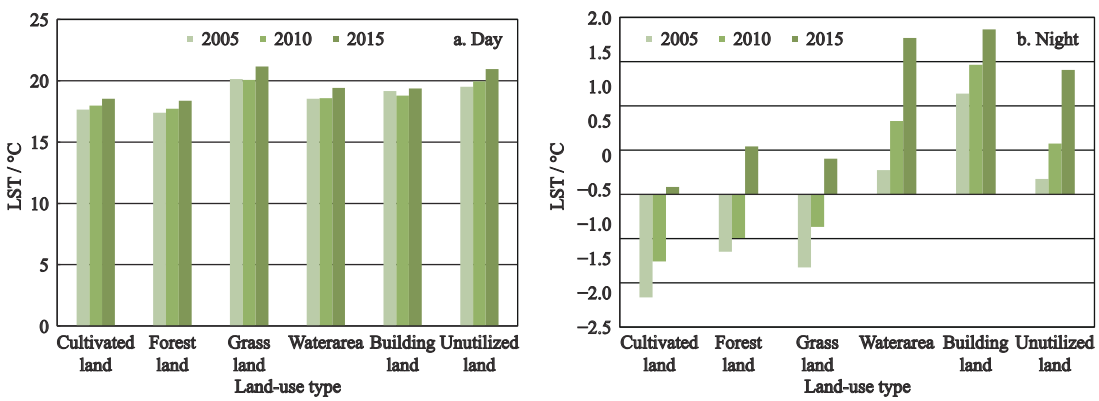

Fig. 6 Diurnal (a) and night (b) annual average land surface temperature (LST) of each land-use type at night from 2005 to 2015 in HBO urban agglomeration, China

largest at night (ΔT = 0.78°C) because heat dissipates faster at night in fallow land, so the temperatures are lower at night.

During 2010–2015, the LST changes that were due to the conversion of grassland to building land were greatest during the daytime (ΔT = 0.85°C) because the grasslands that were converted to building land were mainly medium- and high-cover grasslands in the urban and rural surroundings. The changes in LSTs that were due to converting water areas to building land were greatest at night (ΔT = 1.38°C). For the water area type, it mainly consists beach land that was subsequently converted to building land. Based on protecting the ecological environment, other water areas, such as lakes, ponds and reservoirs, are not suitable for development and construction. Under the climate of arid and semiarid regions, the vegetation coverage of beach land is low, and the temperatures are low at night. Therefore, the LSTs of the water areas that were converted to building land changed greatly.

4 Discussion

4.1 Characteristics of regional heat (cool) island effect of HBO urban agglomerations

From the distribution characteristics of the diurnal RHIIs, we find that the dense building land area in the HBO urban agglomeration exhibits a cool island effect in the daytime and heat island effect in the nighttime, which are similar to the results of existing studies on the heat (cool) island effects of individual cities in arid and semiarid regions (Lazzarini et al., 2013; Mathew et al., 2018; Alahmad et al., 2020). Due to the influence of the climatic background of arid and semiarid regions, their surface vegetation is sparse. Moreover, sandy land, bare land, and other hot land types are widely distributed in suburban areas compared with the high level of vegetation cover in cities, so urban areas exhibit a cool island effect during the daytime. At night, the impermeable surfaces of cities release heat, which causes the surface temperatures to rise and results in a heat island effect.

Compared with the study of the heat island effect of other urban agglomerations, the daytime cool island effect of the HBO urban agglomeration shows a gradual fading trend; that is, the temperature differences between urban and rural areas gradually narrow. The changes in the urban heat island effect at night are relatively stable, but they show a trend from Weak Heat Islands to Strong Heat Islands. Moreover, the heat island effect of the building land-intensive area in the central part of the urban agglomeration at night presents the characteristics of a spatial connection. The existing studies show that with the regional development of urban agglomerations, the heat island effect of a single city in urban agglomerations has spatial overlap and is cross-regional (Han and Xu, 2013). The extents of overlap and connection are related to the degree of development of urban agglomerations, such as the Yangtze River Delta, Pearl River Delta and other mega urban agglomerations. The spatial connections of heat islands are more obvious (Zhang et al., 2017; Lin et al., 2018), while the heat island connection of the Beibu Gulf urban agglomeration (Qin et al., 2020) and Chengdu-Chongqing urban agglomeration is not obvious. In this study, the regional heat island of the HBO agglomeration at night also presents the characteristics of spatial connection. However, this is not significant, which indicates that the urban agglomeration is in a stage of rapid development.

Since 2007, the Inner Mongolia Autonomous Region has begun to cultivate and develop the HBO urban ag-

Table 1 Different land use transition types and their land surface temperature (LST) changes in HBO urban agglomeration, China

Different land use transition	2005–2010			2010–2015		
	Daytime ΔT / °C	Nighttime ΔT / °C	Area / km^2	Daytime ΔT / °C	Nighttime ΔT / °C	Area / km^2
Cultivated to building land	–0.72	0.78	12.83	0.61	1.09	292.06
Forestland to building land	–0.98	0.70	0.03	0.67	1.26	41.95
Grassland to building land	0.45	0.51	18.65	0.85	1.17	607.75
Water area to building land	–	–		0.71	1.38	28.17
Building to building	0.16	0.41	2400.69	0.61	0.91	2413.68
Unutilized land to building land	1.36	0.14	0.72	0.75	1.12	159.21

glomeration and actively promote regional economic integration (Xu and Shi, 2010). The results show that within the HBO urban agglomeration, the warming area of the urban agglomeration is gradually expanding from the eastern region to the central region, which is related to the expansion mode of building land. From 2005 to 2010, the building land in Hohhot in the eastern urban agglomeration expanded relatively rapidly, while from 2010 to 2015, the building land in all cities entered a stage of rapid expansion.

4.2 LST differences in land-use types of HBO urban agglomerations

The land cover characteristics of the HBO urban agglomeration in the context of arid and semiarid climates are different from those of other urban agglomerations. The main land types of the HBO urban agglomeration are grassland and unutilized land, with area shares of 59.35% and 20.80%, respectively. In contrast, the land-use types of other urban agglomerations mainly consist of cultivated land, forestland or building land; for example, the Beijing-Tianjin-Hebei urban agglomeration of China has the largest proportion of cultivated land (47.10%), which is followed by forestland (32.84%), while the Changsha-Zhuzhou-Xiangtan urban agglomeration in Hunan Province of China, has the largest proportion of forestland, which is followed by cultivated land.

There are differences in the LSTs between different land-use types, and studies have shown that forestland and cultivated land are low-temperature land types and that building land is a high-temperature land type (Sun et al., 2018). The same conclusion was also reached in this paper. However, unlike the conclusions of other studies, the unutilized land in the HBO urban agglomeration is a high-temperature land type. Among the types of unutilized land, the LSTs of sandy land, saline land, and marshland vary widely, with lower LSTs for marshland and higher LSTs for sandy land. In other urban agglomeration studies, grassland is mostly categorized as green land, which is a land type that has a mitigating effect on the urban heat island effect. In arid and semiarid urban agglomerations, grasslands are classified as high-temperature land types. Among the grassland types, grasslands with different vegetation cover have significantly different LSTs, and grasslands have high cover and lower LSTs.

In studies of the individual UHI effects in arid and semiarid regions, the land use types in rural areas mostly have high LSTs (e.g., bare land and low vegetation cover), which are attributed to the emergence of urban cold island effects (Mohammad et al., 2019; Naserikia et al., 2019; Bindajam et al., 2020). Similar to the results from individual cities, the suburban extent of the HBO urban agglomeration mainly consists of high-temperature land-use types. In contrast, the suburban extents of other urban agglomerations consist of low-temperature land-use types. Due to the differences in climate, the higher LSTs in the suburban areas of the HBO urban agglomeration than in the urban areas during the daytime show a cool island effect. In contrast, the other urban agglomerations show a heat island effect.

4.3 Shortcomings and prospects

In terms of the research methods, the calculation methods for the heat island intensities in current heat island studies of urban agglomerations have not yet been unified, and each method has advantages and disadvantages. The RHII calculation method referenced in this paper has the advantage of simplicity, which uses the overall cultivated land in the study area as the rural background and excludes the interference from topography and human factors. However, the method ignores intercity microclimates, which thus affects the LST values of the rural background, which is an unavoidable problem in regional urban heat islands. Studies at regional scales should be based on regional climate backgrounds, and the HBO urban agglomeration belongs to the semiarid continental monsoonal steppe climate, which has similar climate characteristics, so the method is considered to be applicable to this study area. In the process of RHII estimations, the errors in the interannual LST data, which were obtained by the averaging method in this paper, also need to be considered. Although the 8-d synthetic LSTs exclude the influences of cloudiness and other factors to ensure the quality of each image, the errors arising from averaging twice need to be considered. Existing studies also address the problem of missing data due to cloud cover in remote sensing images by using methods such as random forest regression (Zhao and Duan, 2020), satellite thermal infrared and satellite passive microwave measurements (Duan et al., 2017) to reconstruct the LST, and the reconstructed LST is closer to the actual value, which can

be used in future studies to process the LST data will achieve better results.

In the research content, we only studied the interannual RHI characteristics of the HBO urban agglomeration and briefly explored the relationships among the land use types and LSTs without going deeply into analyzing the influencing factors of RHI in the HBO urban agglomeration. Future studies should add biophysical, socioeconomic and meteorological factors and analyze the contributions of these impact factors to the RHII.

5 Conclusions

In this study, the MOD11A2 8-d synthetic surface temperature data and land use classification data for 2005, 2010 and 2015 were used as the main data, as well as the DMSP/OLS nighttime light data and DEM elevation data, to extract the rural background. Then, the RHIIs were calculated and used to classify the heat island class. We analyzed the spatial and temporal distribution characteristics of the RHIs in the HBO urban agglomeration and explored the effects of building land-use changes on surface temperatures. The main conclusions are as follows.

(1) The spatial and temporal distribution characteristics of diurnal RH(C)I in urban agglomeration have large differences. During the daytime, cold islands are mainly distributed in the eastern, northern and central areas, and heat islands are mainly distributed in the desert areas in the west and southwest; at night, cold islands are mainly distributed in the northern and central-western areas of the urban cluster, and heat islands are mainly distributed in the central, northwestern and southern areas. Among them, the diurnal RH(C)I in the central part of the HBO urban agglomeration, where building land is densely distributed, has the largest variation from 2005 to 2015. During the daytime, the central part of the urban cluster shows a trend of change from Weak Cool Island to No Heat Island, and the area of No Heat Island expands; at night, Strong Heat Island and Weak Heat Island are mainly distributed in the central part of the urban agglomeration, and the heat island area as a whole shows a change characteristic of first decreasing and then increasing. It can be seen that urbanization activities have a great influence role on the spatial and temporal distribution and evolution of RH(C)I.

(2) The surface temperatures for each land use type during the day are grassland > unutilized land > building land > water area > cultivated land > forestland; the surface temperatures for each land use type at night are building land > water area > unutilized land > forestland > grassland > cultivated land.

(3) From 2005 to 2010, the land-use changes had a greater impact on the daytime surface temperature changes, while the land-use changes from 2010 to 2015 had a greater impact on the nighttime surface temperature changes. During 2005−2010, the temperature of unused land that was converted to building land changed the most during the day (ΔT = 1.36°C), and those of dry land that was converted to building land changed the most at night (ΔT = 0.78°C). From 2010 to 2015, the temperature of grassland that was converted to construction land changed the most during the day (ΔT = 0.85°C), and those of water areas that was converted to building land changed the most at night (ΔT = 1.38°C).

References

Akbari H, Kolokotsa D, 2016. Three decades of urban heat islands and mitigation technologies research. *Energy and Buildings*, 133: 834–842. doi: 10.1016/j.enbuild.2016.09.067

Alahmad B, Tomasso L P, Al-Hemoud A et al., 2020. Spatial distribution of land surface temperatures in kuwait: urban heat and cool islands. *International Journal of Environmental Research and Public Health*, 17(9): 2993. doi: 10.3390/ijerph17092993

Bindajam A A, Mallick J, Alqadhi S et al., 2020. Impacts of vegetation and topography on land surface temperature variability over the semi-arid mountain cities of saudi arabia. *Atmosphere*, 11(7): 762. doi: 10.3390/atmos11070762

Bonafoni S, Baldinelli G, Verducci, 2017. Sustainable strategies for smart cities: analysis of the town development effect on surface urban heat island through remote sensing methodologies. *Sustainable Cities and Society*, 29: 211–218. doi: 10.1016/j.scs.2016.11.005

Debbage N, Shepherd J M, 2015. The urban heat island effect and city contiguity. *Computers, Environment and Urban Systems*, 54: 181–194. doi: 10.1016/j.compenvurbsys.2015.08.002

Du H Y, Wang D D, Wang Y Y et al., 2016. Influences of land cover types, meteorological conditions, anthropogenic heat and urban area on surface urban heat island in the yangtze river delta urban agglomeration. *Science of the Total Environment*, 571: 461–470. doi: 10.1016/j.scitotenv.2016.07.012

Duan S B, Li Z L, Leng P, 2017. A framework for the retrieval of all-weather land surface temperature at a high spatial resolution from polar-orbiting thermal infrared and passive microwave data. *Remote Sensing of Environment*, 195: 107–117. doi: 10.1016/j.rse.2017.04.008

Fang Chuanglin, Zhou Chenghu, Gu Chaolin et al., 2016. Theor-

etical analysis of interactive coupled effects between urbanization and eco-environment in mega-urban agglomerations. *Acta Geographica Sinica*, 71(4): 531–550. (in Chinese)

Fu P, Weng Q H, 2016. A time series analysis of urbanization induced land use and land cover change and its impact on land surface temperature with Landsat imagery. *Remote Sensing of Environment*, 175: 205–214. doi: 10.1016/j.rse.2015.12.040

Gao J, Yu Z W, Wang L C et al., 2019. Suitability of regional development based on ecosystem service benefits and losses: a case study of the Yangtze River Delta urban agglomeration, China. *Ecological Indicators*, 107: 105579. doi: 10.1016/j.ecolind.2019.105579

Ge Weiqiang, Zhou Hongmei, Yang Hequn, 2010. Characteristics analysis on heat island effect in Yangtze Delta urban agglomerations in recent 8 years by MODIS data. *Meteorological Monthly*, 26(11): 77–81. (in Chinese)

Haashemi S, Weng Q H, Darvishi A et al., 2016. Seasonal variations of the surface urban heat island in a semi-arid city. *Remote Sensing*, 8(4): 352. doi: 10.3390/rs8040352

Han G F, Xu J H, 2013. Land surface phenology and land surface temperature changes along an urban-rural gradient in Yangtze River Delta, China. *Environmental Management*, 52(1): 234–249. doi: 10.1007/s00267-013-0097-6

Inner Mongolia Autonomous Region Statistics Bureau, 2016. *Inner Mongolia Statistical Yearbook* 2015.

Jahangir M S, Moghim S, 2019. Assessment of the urban heat island in the city of tehran using reliability methods. *Atmospheric Research*, 225: 144–156. doi: 10.1016/j.atmosres.2019.03.038

Lazzarini M, Marpu P R, Ghedira H, 2013. Temperature-land cover interactions: the inversion of urban heat island phenomenon in desert city areas. *Remote Sensing of Environment*, 130: 136–152. doi: 10.1016/j.rse.2012.11.007

Lemoine-Rodríguez R, Inostroza L, Zepp H, 2022. Intraurban heterogeneity of space-time land surface temperature trends in six climate-diverse cities. *Science of the Total Environment*, 804: 150037. doi: 10.1016/j.scitotenv.2021.150037

Li W F, Han C M, Li W J et al., 2020. Multi-scale effects of urban agglomeration on thermal environment: a case of the Yangtze River Delta Megaregion, China. *Science of the Total Environment*, 713: 136556. doi: 10.1016/j.scitotenv.2020.136556

Liao D Q, Zhu H N, Jiang P, 2021. Study of urban heat island index methods for urban agglomerations (hilly terrain) in Chongqing. *Theoretical and Applied Climatology*, 143(1): 279–289. doi: 10.1007/s00704-020-03433-8

Lin Zhongli, Xu Hanqiu, Chen Hong, 2018. Urban heat island change and its relationship to the urbanization of three major urban agglomerations in China's eastern coastal region. *Research of Environmental Sciences*, 31(10): 1695–1704. (in Chinese)

Luintel N, Ma Weiqiang, Ma Yaoming et al., 2019. Spatial and temporal variation of daytime and nighttime MODIS land surface temperature across Nepal. *Atmospheric and Oceanic Science Letters*, 12(5): 305–312. doi: 10.1080/16742834.2019.1625701

Majumder A, Setia R, Kingra P K et al., 2021. Estimation of land surface temperature using different retrieval methods for studying the spatiotemporal variations of surface urban heat and cold islands in indian punjab. *Environment, Development and Sustainability*, 23(11): 15921–15942. doi: 10.1007/s10668-021-01321-3

Mathew A, Khandelwal S, Kaul N, 2018. Analysis of diurnal surface temperature variations for the assessment of surface urban heat island effect over Indian cities. *Energy and Buildings*, 159: 271–295. doi: 10.1016/j.enbuild.2017.10.062

Mohammad P, Goswami A, Bonafoni S, 2019. The impact of the land cover dynamics on surface urban heat island variations in semi-arid cities: a case study in Ahmedabad City, India, using multi-sensor/source data. *Sensors*, 19(17): 3701. doi: 10.3390/s19173701

Naserikia M, Asadi Shamsabadi E, Rafieian M et al., 2019. The urban heat island in an urban context: a case study of Mashhad, Iran. *International Journal of Environmental Research and Public Health*, 16(3): 313. doi: 10.3390/ijerph16030313

Oleson K W, Monaghan A, Wilhelmi O et al., 2015. Interactions between urbanization, heat stress, and climate change. *Climatic Change*, 129(3–4): 525–541. doi: 10.1007/s10584-013-0936-8

Peng J, Xie P, Liu Y X et al., 2016. Urban thermal environment dynamics and associated landscape pattern factors: a case study in the Beijing metropolitan region. *Remote Sensing of Environment*, 173: 145–155. doi: 10.1016/j.rse.2015.11.027

Peng S S, Piao S L, Ciais P et al., 2012. Surface urban heat island across 419 global big cities. *Environmental Science & Technology*, 46(2): 696–703. doi: 10.1021/es2030438

Qiao Zhi, Tian Guangjin, 2015. Dynamic monitoring of the footprint and capacity for urban heat island in Beijing between 2001 and 2012 based on MODIS. *Journal of Remote Sensing*, 19(2): 476–484. (in Chinese)

Qin Menglin, Song Wenbo, Song Yuanzhen et al., 2020. Study on spatial features and evolutionary trend of heat islands in Beibu Gulf urban agglomeration. *Journal of Safety and Environment*, 20(4): 1557–1566. (in Chinese)

Quintana-Talvac C, Corvacho-Ganahin O, Smith P et al., 2021. Urban heat islands and vulnerable populations in a mid-size coastal city in an arid environment. *Atmosphere*, 12(7): 917. doi: 10.3390/atmos12070917

Rasul A, Balzter H, Smith C et al., 2017. A review on remote sensing of urban heat and cool islands. *Land*, 6(2): 38. doi: 10.3390/land6020038

Seto K C, Güneralp B, Hutyra L R, 2012. Global forecasts of urban expansion to 2030 and direct impacts on biodiversity and carbon pools. *Proceedings of the National Academy of Sciences of the United States of America*, 109(40): 16083–16088. doi: 10.1073/pnas.1211658109

Song Yongyong, Xue Dongqian, Ma Beibei et al., 2020. Urbanization process and its ecological environment response pattern

on the Loess Plateau, China. *Economic Geography*, 40(6): 174–184. (in Chinese)

Stewart I D, 2011. A systematic review and scientific critique of methodology in modern urban heat island literature. *International Journal of Climatology*, 31(2): 200–217. doi: 10.1002/joc.2141

Sun Y, Hu T, Zhang X B et al., 2019. Contribution of global warming and urbanization to changes in temperature extremes in eastern China. *Geophysical Research Letters*, 46(20): 11426–11434. doi: 10.1029/2019gl084281

Sun Zongyao, Sun Xihua, Xu Xinliang et al., 2018. Study on the contribution of land use heterogeneity and change to regional thermal environment: a case study of Beijing-Tianjin-Hebei urban agglomeration. *Ecology and Environmental Sciences*, 27(7): 1313–1322. (in Chinese)

Taha H, 1997. Urban climates and heat islands: albedo, evapotranspiration, and anthropogenic heat. *Energy and Buildings*, 25(2): 99–103. doi: 10.1016/S0378-7788(96)00999-1

UN-Habitat, 2016. *Urbanization and Development*: *Emerging Futures*. Nairobi: UN-Habitat.

United Nations, Department of Economiical and Social Affairs, 2018. *World Urbanization Prospects*: *The 2018 Revision*, *Highlights*. New York: United Nations.

Wang C H, Wang Z H, Li Q, 2020a. Emergence of urban clustering among U. S. cities under environmental stressors. *Sustainable Cities and Society*, 63: 102481. doi: 10.1016/j.scs.2020.102481

Wang Z Y, Liu M L, Liu X N et al., 2020b. Spatio-temporal evolution of surface urban heat islands in the Chang-Zhu-Tan urban agglomeration. *Physics and Chemistry of the Earth, Parts A/B/C*, 117: 102865. doi: 10.1016/j.pce.2020.102865

Wu X J, Wang G X, Yao R et al., 2019. Investigating surface urban heat islands in south america based on MODIS data from 2003 –2016. *Remote Sensing*, 11(10): 1212. doi: 10.3390/rs11101212

Wu Z F, Xu Y, Cao Z et al., 2021. Impact of urban agglomeration and physical and socioeconomic factors on surface urban heat islands in the Pearl River Delta Region, China. *IEEE Journal of Selected Topics in Applied Earth Observations and Remote Sensing*, 14: 8815–8822. doi: 10.1109/JSTARS.2021.3108456

Xu Jing, Shi Ligao, 2010. Spatial motive mechanism and integrative development mode of Hohhot-Baotou-Ordos region. *Journal of Arid Land Resources and Environment*, 24(7): 52–57. (in Chinese)

Yao R, Wang L C, Huang X et al., 2017. Temporal trends of surface urban heat islands and associated determinants in major Chinese cities. *Science of the Total Environment*, 609: 742–754. doi: 10.1016/j.scitotenv.2017.07.217

Yu Z W, Yao Y W, Yang G Y et al., 2019a. Spatiotemporal patterns and characteristics of remotely sensed region heat islands during the rapid urbanization (1995–2015) of Southern China. *Science of the Total Environment*, 674: 242–254. doi: 10.1016/j.scitotenv.2019.04.088

Yu Z W, Yao Y W, Yang G Y et al., 2019b. Strong contribution of rapid urbanization and urban agglomeration development to regional thermal environment dynamics and evolution. *Forest Ecology and Management*, 446: 214–225. doi: 10.1016/j.foreco.2019.05.046

Yuan W H, Li J C, Meng L et al., 2019. Measuring the area green efficiency and the influencing factors in urban agglomeration. *Journal of Cleaner Production*, 241: 118092. doi: 10.1016/j.jclepro.2019.118092

Yun G Y, Ngarambe J, Duhirwe P N et al., 2020. Predicting the magnitude and the characteristics of the urban heat island in coastal cities in the proximity of desert landforms. The case of Sydney. *Science of the Total Environment*, 709: 136068. doi: 10.1016/j.scitotenv.2019.136068

Zhang Shuo, Liu Yonghong, Huang Hongtao, 2017. Research on quantitative evaluations and spatial and temporal distribution of heat islands for the Pearl River Delta agglomeration. *Ecology and Environmental Sciences*, 26(7): 1157–1166. (in Chinese)

Zhao W, Duan S B, 2020. Reconstruction of daytime land surface temperatures under cloud-covered conditions using integrated modis/terra land products and msg geostationary satellite data. *Remote Sensing of Environment*, 247: 111931. doi: 10.1016/j.rse.2020.111931

Zhou D C, Li D, Sun G et al., 2016. Contrasting effects of urbanization and agriculture on surface temperature in eastern China. *Journal of Geophysical Research*, 121(16): 9597–9606. doi: 10.1002/2016JD025359

Zhuang Yuan, Xue Dongqian, Kuang Wenhui et al., 2019. Study on the pattern of land cover hierarchy in hohhot-baotou- ordos cities in the semi-arid region of China. *Remote Sensing Technology and Application*, 34(1): 197–206. (in Chinese)